

A New Approach to Ultrasonic Degassing to Improve the Mechanical Properties of Aluminum Alloys

H. Puga, J. Barbosa, J.C. Teixeira, and M. Prokic

(Submitted February 24, 2014; in revised form June 4, 2014; published online July 8, 2014)

Ultrasonic degassing of liquid metals has been studied over the last years, but it has been limited to laboratorial scale experiments of low volumes of melt. In this work, the combined effect of acoustic cavitation with metal agitation induced by the mechanical vibration of the ultrasonic radiator itself was studied, using a specially designed low frequency mechanical vibrator coupled to the ultrasonic degassing unit. Liquid motion in water was characterized by high speed digital Photron—FastCam APX RS video camera and Laser Doppler Anemometry to select the most favorable US and mechanical vibrator frequencies to induce suitable water stirring. Selected parameters were used to degas 10 L of AlSi9Cu3(Fe) alloy. A suitable piezoelectric sensor was used to measure sound pressure at different distances from the sonotrode to identify the zone of higher acoustic activity. Results have shown that melt stirring significantly improves US degassing efficiency (since it is possible to achieve almost the aluminum alloy theoretical density after 3 min processing time) which contributed to increase the tensile properties of the alloy.

Keywords aluminum alloy, casting, cavitation, mechanical properties, ultrasonic

1. Introduction

The application of ultrasonic vibrations for casting of aluminum, magnesium, and steel alloys is known to be a non-complex technology which can improve the final quality of castings. Ultrasound has been used with different purposes in metal casting: (1) Degassing of aluminum and magnesium alloys leading to high density and virtually gas porosity free casting (Ref 1, 2); (2) promoting nucleation, thus leading to highly refined microstructures (Ref 3, 4); (3) improving castings mechanical properties either by promoting heterogeneous nucleation and development of equiaxed globular structures (Ref 5) or dendrite fragmentation (Ref 5, 6); and (4) promoting homogeneous dispersion in aluminum metal matrix composites (Ref 7).

The physical mechanism of degassing aluminum alloys through ultrasonic vibration devices is a research area which has been receiving relevant attention over the last few decades (Ref 1, 8, 9). Many ultrasonic devices capable of automatic generation of waves and integration of different bodies have been developed. The various approaches to promote reduction of hydrogen dissolved in the liquid tend to differ in the principle used to generate wave (e.g., magneto or piezoelectric system), in the frequency selection method (e.g., constant or adjustable), and in the shape of the propagated wave (e.g., radial or planar).

In order to describe the movement of a wave in a liquid medium, it is necessary to establish a relation between disturbance, time, and distance to the source of oscillation. Thus, an elastic wave propagation in a fluid represents an alternating flow and obeys the hydrodynamic laws, which can be written as Eq 1 (Ref 10)

$$f(\rho, p_a, T) = 0, \quad (\text{Eq 1})$$

where ρ and p_a are the density and acoustic pressure, respectively, and T the medium temperature.

Physically, elastic oscillations can occur both in the range of audio, ultrasonic, or hypersonic frequencies. However, phenomena such as acoustic cavitation and flows in the ultrasonic range are considered the most important for melt treatment in the scope of metallurgy (Ref 6, 11).

For an effective degassing the acoustic energy supplied to the melt must have sufficient intensity (I) to promote enough pressure to induce the cavitation phenomenon (Ref 12) that can be explained as follows: when a liquid metal is submitted to high intensity ultrasonic vibrations, the alternating pressure above the cavitation threshold creates numerous cavities in the liquid metal (Ref 10, 13) which intensifies mass transfer processes and accelerates the diffusion of hydrogen from the melt to the developed bubbles. As acoustic cavitation progresses in time, adjacent bubbles touch and coalesce, growing to a size sufficient to allow them to rise up through the liquid, against gravity, until they reach the surface (Ref 10, 13). However, some bubbles which are not filled with gas tend to collapse during the compression cycle, before reaching the liquid surface, which causes the acoustic streaming phenomenon as well as new nucleation sites (Ref 10). When submitting a liquid media to ultrasound, direct hydrodynamic flows in melts. These flows are usually called acoustic streams that occur both in the bulk of the liquid and near the walls, particles, and other inclusions or objects within oscillating ultrasonic fields. The origin of those streams relates to the ultrasonic momentum acquired by the liquid media when it absorbs the

H. Puga, J. Barbosa, and J.C. Teixeira, Centre for Mechanical and Materials Technologies (CT2M), Universidade do Minho, Azurém, 4800-058 Guimarães, Portugal; and M. Prokic, MP Interconsulting, 2400 Le Locle, Switzerland. Contact e-mail: puga@dem.uminho.pt.

wave, Therefore, the velocity of acoustic streams increases with the ultrasonic intensity and the sound absorption (Ref 8).

The efficiency of ultrasonic treatment (UST) depends on many factors, namely the ultrasonic parameters, such as amplitude and frequency of vibration, the degassing conditions (melt treatment temperature and time), the alloy composition, and the material purity and volume, all of great importance in the obtained results (Ref 1, 2, 14).

Besides, it is known that one of the main factors affecting the efficiency of UST is the acoustic intensity, which can be determined by Eq 2 for the simplest case of a plane traveling wave (Ref 10), i.e., power flux (P) divided by area (S) or volume (V) in which these component, area or volume, are dependent of the approach used to propagate the waves in the medium

$$I = \frac{P}{S \text{ (or) } V}, \quad (\text{Eq 2})$$

Acoustic intensity can be used to predict the extent to which acoustic cavitation is developed in the medium. However, acoustic intensity tends to decrease exponentially with the propagation in the path x , due to energy loss in the medium in accordance with the Eq 3 (Ref 10)

$$I = I_0 e^{-2\alpha x}, \quad (\text{Eq 3})$$

where α is the acoustic attenuation, which can be caused by the phenomena of absorption associated to viscous loss (loss in the medium) and the phenomena of dispersion related to the heterogeneity of the medium (loss in the boundary), which is more evident in small volumes (stationary medium).

Extensive field tests conducted by experts in this field have demonstrated that in order to achieve high efficiency, the ultrasonic systems must be well tuned to the load (Ref 10, 11, 15) and applied to a small volume of melt.

Industrially, the great interest in ultrasonic degassing of aluminum alloys is particularly important in stationary and medium or large melt volumes, where acoustic attenuation may represent an important factor on the degassing efficiency, or in melts with high hydrogen content (Ref 16). Under those conditions, the cavitation effect may be limited to a small volume of melt near the acoustic radiator. Thus, a possible way to overtake such drawback/limitation is to induce a gentle motion to the liquid media, usually called melt stirring, in order to make it pass through the region where cavitation intensity is higher and better developed, thus increasing the quantity of melt submitted to cavitation. In this case, the mechanical melt stirring needs to be smooth enough to avoid turbulence at the melt surface to avoid new absorption of hydrogen.

The main goal of the present work was to study the effect of acoustic cavitation combined with a low frequency mechanical vibrator in the motion of the liquid medium in the field of ultrasonic sonochemistry, using an ultrasonic degassing apparatus based on the MMM (Multi-frequency Multimode Modulated ultrasonic technology). For that purpose, a suitable US degassing design coupled to a low frequency mechanical vibrator was developed, tested, and evaluated in water and liquid AlSi9Cu3(Fe).

2. Materials and Experimental Procedures

This work is focused on two different stages, according to the envisaged objective:

- (1) Evaluation and characterization of the optimal processing conditions in water medium (frequency of the mechanical vibrator for a pre-established ultrasonic frequency of ultrasound) that lead to the maximum water stirring action.
- (2) Characterization of the degassing efficiency and mechanical properties in AlSi9Cu3(Fe) melts, using the best processing conditions established for water medium.

2.1 Material

The composition of the commercially available AlSi9Cu3(Fe) alloy used in this work was evaluated by Optical Emission Spectrometry and it consisted of Al-9.15Si-2.25Cu-0.18Mg-0.66Fe-0.26Mn-0.47Zn-0.25Sn.

2.2 Experimental Procedures

To evaluate and characterize the optimal processing conditions in stage 1, the study was divided in two main steps: (1) study of the simple effect of the low frequency mechanical vibrator on the movement of the acoustic radiator, using 15, 20, 30, and 35 Hz; (2) study of the flux movement induced by an oscillatory motion in the surrounding fluid (water) using simultaneously the low frequency mechanical vibrator and the ultrasonic radiator. The ultrasonic system for liquid aluminum/water processing used in this research consists of a high power ultrasonic converter, an acoustic wave-guide, and an acoustic radiator (or sonotrode) 600 mm long and 60 mm in diameter, driven by wideband, frequency modulated ultrasonic signal from MMM ultrasonic power supply unit, developed by MP Interconsulting (Ref 15). In addition, a low frequency mechanical vibrator was coupled to the acoustic radiator by a flexible

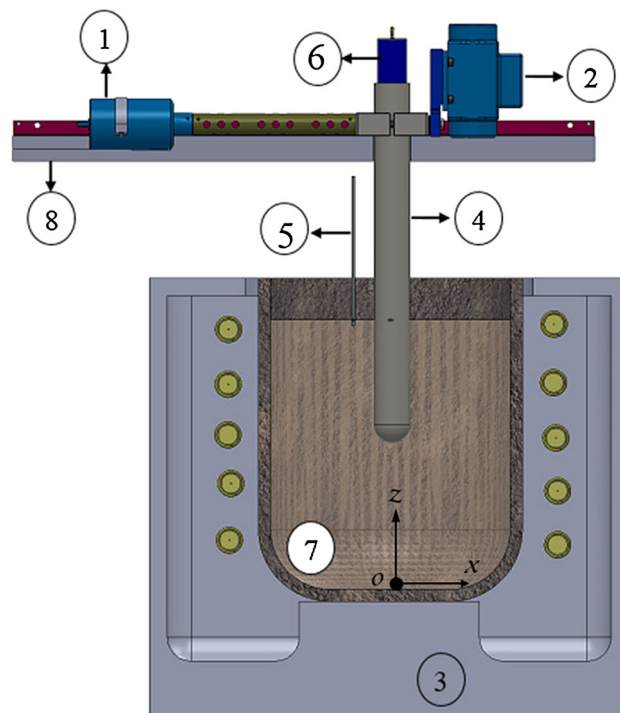


Fig. 1 MMM ultrasonic system—conceptual model: 1—transducer; 2—low frequency mechanical vibrator; 3—furnace; 4—acoustic radiator; 5—thermocouple; 6—air cooling tube; 7—molten aluminum alloy; and 8—protection box

mechanical interface in order to create helical vibrations, as shown in Fig. 1.

The MMM technology is characterized by synchronously exciting many (mutually coupled) vibration modes and harmonics of ultrasonic system, which will be sent to solid and liquid media. This technology produces high intensity multi-mode vibrations that are spatially uniform and repeatable, while avoiding creation of stationary and standing waves. This way, the whole vibrating system (including its liquid aluminum load) is fully and uniformly agitated, improving homogenization, degassing, and even grain refinement, while increasing density and removing non-metallic inclusions. The ultrasonic power supply unit is fully controlled by dedicated Windows compatible (Lab View) software developed by MPI. Relevant ultrasonic parameters in this process are frequency sweeping interval, sweeping frequency repetition rate, f_{swm} (controllable frequency shift with modulation) for the selected resonance frequency interval and output electric power. Mentioned parameters are adjusted in order to produce the highest acoustic amplitude and a sufficiently wide frequency spectrum in a liquid metal, automatically monitored with a specifically implemented feedback loop. Although the ultrasonic apparatus has the capability to work on a pulsatory regime, in what this work is concerned it has worked continuously.

In step (1), a high speed digital Photron—FastCam APX RS video camera capable of 10,000 fps at 1 M pixel was used, according to Fig. 2(a). The video sequences were recorded at 1000 fps and subsequently image analysis TEMA Motion software was used to determine the motion in function of time. A mark was placed at the radiator surface and a scale was visible in order to calibrate the frames. In this stage, ultrasound was not being supplied to the melt.

In step (2), the two best frequencies of the mechanical vibrator (15 and 35 Hz) selected in step (1) were used simultaneously with 19.8 ± 0.1 kHz US frequency and 60% of US electric power to evaluate the flux profile induced in the surrounding fluid. For that purpose, the radiator was placed in a circular vessel, 200 mm in diameter and 240 mm in height, filled with water at $18 \pm 1^\circ\text{C}$ up to 200 mm height, and deepen 110 mm in the water. In order to reduce optical distortion, the circular vessel was placed inside a square vessel also filled with water. This way the mismatch of refractive indexes at the curved interface is reduced. The velocity field was measured by a two-component DANTEC Laser Doppler Anemometry (LDA) with a spatial resolution of approximately 1 mm, according to Fig. 2(b). The Doppler signals were processed in the frequency domain by Burst Spectrum Analyzers. 20- μm polystyrene tracer particles were used as a diffracting medium for the laser beams. For each position in the fluid, the average velocity was statistically determined from 3000 samples. This way, the velocity profile in the vicinity of the radiator was determined. Table 1 presents the main parameters of the laser and the mesh parameters of the measured volume.

Table 1 Main parameters of the measurement volume

Parameters of measurement volume		
	Green beam	Blue beam
Angle diffraction (2θ)	19.382	19.502
Control mesh (mm)	Radius _{radiator} – Radius _{glass container}	
x	$y = 0$ (C^{te} along of path y)	
y	$z = 10; z = 50; z = 90$	
z		

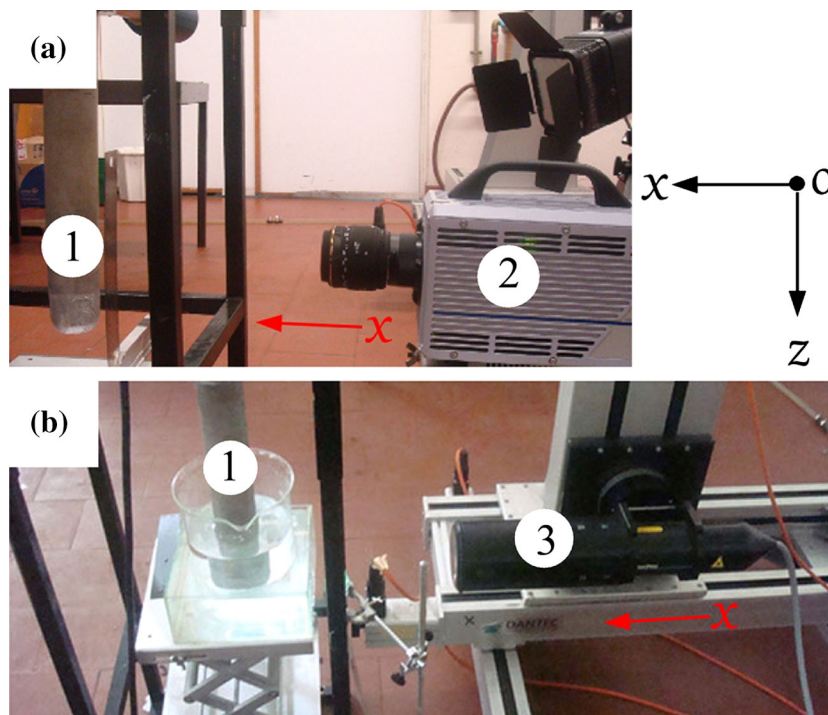


Fig. 2 (a) Experimental apparatus to measure the displacement amplitude of the acoustic radiator; (b) experimental apparatus to characterize the velocity profile due to the combined effect of mechanical and US vibration. 1—Sonotrode; 2—high speed digital Photron; and 3—DANTEC Laser Doppler Anemometry

In stage 2, after the evaluation and selection of the best processing conditions in water, a 10 L molten bath of AlSi9Cu3(Fe) alloy was produced in a resistance furnace equipped with a 230 mm diameter and 290 mm height SiC crucible. Melt temperatures of 660 and 700°C within an accuracy of $\pm 10^\circ\text{C}$ were used to perform degassing tests, using the parameters selected in stage 1. For the sake of comparison, argon degassing (injection flow of 5 l/min) using the rotary diffuser technique at 100 rpm from 0 to 5 min was also performed at the same temperatures. Samples for mechanical characterization were cylinders with 14 mm in diameter and 140 mm length, obtained by pouring the molten alloy into a metallic die at 200°C melt temperature.

2.3 Physical Modeling

Water is considered a suitable media to simulate the US degassing mechanism in liquid aluminum alloys (Ref 10). Moreover, as the dynamic viscosity of water at room temperature is similar to the molten aluminum alloy, phenomena in isothermal water modeling are considered to be dominated only by inertial and gravitational forces, therefore dynamic similarity is achieved when the ratio of the inertial to the buoyancy forces in both systems is similar (Ref 18).

The methodology for physical modeling the liquid medium motion caused by acoustic cavitation combined with low frequency mechanical vibration results from the theory of similarity on which criteria of geometric and dynamic features were considered. In what concerns to geometric similarity the following relation was assumed:

$$\left(\frac{\phi}{h}\right)_{\text{model}_w} = \left(\frac{\phi}{h}\right)_{\text{model}_{Al}} \approx 1, \quad (\text{Eq 4})$$

where ϕ and h represent the diameter of the container and height of the fluid, respectively. Apart from these characteristics, the ultrasound device was the same in the different stages of the present work. Thus, the apparatus used for research was built in a scale of one-to-one (1:1) capable of predicting the best processing conditions in water medium to apply in molten aluminum alloy.

The Froude number (Fr) that relates the inertial and gravitational forces, was considered as dynamic similarity criteria to correlate the flux movement induced by an oscillatory motion in the surrounding fluid between the model in water and in molten aluminum alloy, as used by other authors (Ref 18, 19). Thus, in a one-to-one model, both the reference fluid length (L) and velocity (v) will be the same for free surface. So, since the Froude number does not contain any fluid properties it was considered that

$$Fr_{\text{model}_w} = \frac{v}{\sqrt{gL}} = Fr_{\text{model}_{Al}}, \quad (\text{Eq 5})$$

is automatically satisfied in a one-to-one model.

2.4 Evaluation of Hydrogen Content in the Aluminum Melt

Melt samples for characterization were taken immediately before starting the degassing operation and after 1, 3, and 5 min of ultrasonic processing, for each processing parameters combination. Hydrogen content evaluation was performed using the traditional ‘‘Straube-Pfeiffer’’ method, also known as reduced pressure test (RPT). The molten alloy was poured into a thin-wall iron cup (≈ 120 g) and allowed to solidify

under a reduced pressure of 70 mmHg. Its density (d) was evaluated by the apparent density measurement technique, using the following equations (Ref 17):

$$d = \frac{W_a}{W_a - W_w}, \quad (\text{Eq 6})$$

where W_a and W_w are the sample weights measured in air and water, respectively. The volume of gas (V_g) was given by Eq 7, where d_0 is the alloy theoretical density and k is a constant for standard temperature and pressure conditions correction, given by Eq 8

$$V_g = k \times \left(\frac{1}{d} - \frac{1}{d_0}\right), \quad (\text{Eq 7})$$

$$k = \left(\frac{\text{Test pressure}}{760}\right) \times \left(\frac{273}{273 + \text{alloy freezing temperature}}\right). \quad (\text{Eq 8})$$

2.5 Evaluation of Mechanical Properties

For tensile testing, the specimens were machined from the as-cast samples according to EN10002-1:2004 with gage length L_0 of 50 mm and cross section diameter d_0 of 10 mm. Tensile tests were carried out at room temperature in an INSTRON-Model 8874 testing machine using 0.5 mm/min strain rate to obtain yield strength, ultimate tensile strength, and strain.

3. Results and Discussion

3.1 Experiments in Water Medium

In the first stage, in order to evaluate and characterize the optimal processing conditions in water medium (frequency of the mechanical vibrator for a pre-established ultrasonic frequency of ultrasound), the individual effect of the low frequency mechanical vibrator in the movement of the acoustic radiator was studied (step 1). Figure 3 shows the variation in the maximum amplitude of the acoustic radiator for 15, 20, 30, and 35 Hz frequencies.

In order to simplify results presentation only 0.5 s of the recorded spectra are presented. However, according to these results it can be seen that the motion is repetitive in time. As shown in Fig. 3(a) to 3(d), the amplitude of movement tends to increase in both Ox and Oz direction. By comparing Fig. 3(b) and 3(c), it is clear that there is an inversion of the amplitudes in the Ox and Oz direction. After a series of trials for frequencies between 20 and 30 Hz and different equipment holding systems, it was concluded that the most important factor in that amplitude inversion effect was the equipment holding conditions, i.e., for the adopted conditions in this frequency interval (20-30 Hz) the system presented natural resonance frequency.

For this reason experiments in step (2) were carried out using 15 and 35 Hz frequencies of the mechanical vibrator in combination with $19,800 \pm 0.25$ Hz ultrasonic frequency. The flux profile created by the combined effects was investigated under both Ox and Oz paths at three different heights from the base of the water container ($Z = 10$ mm, $Z = 50$ mm, and $Z = 90$ mm), according to the adopted coordinate system shown in Fig. 2.

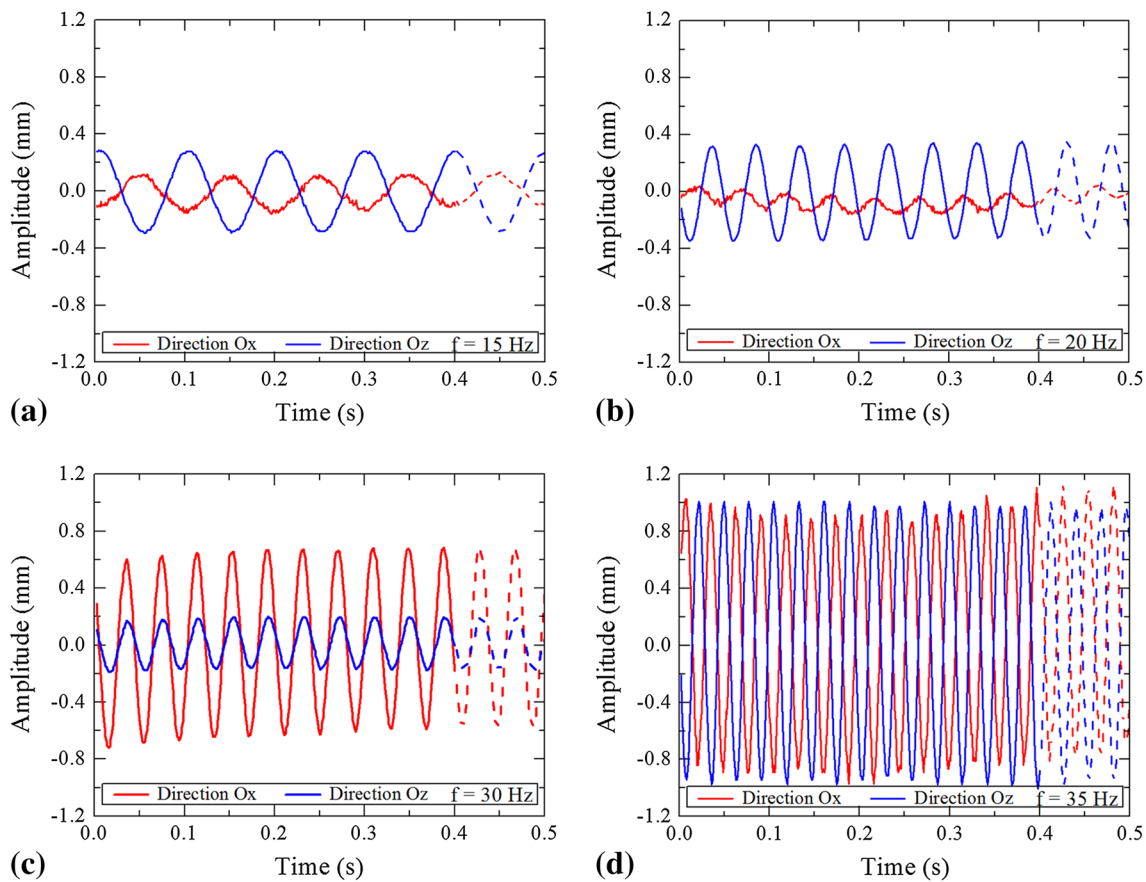


Fig. 3 Effect of low frequency mechanical vibration in the movement of the acoustic radiator: (a) $f = 15$ Hz; (b) $f = 20$ Hz; (c) $f = 30$ Hz; and (d) $f = 35$ Hz

Figure 4 shows the dimensionless velocity ratio (v/v_{\max}) in the Ox and Oz paths promoted by the combination of both effects at different distances from the base of the water vessel. v represents the velocity at the point and v_{\max} the maximum velocity registered in the liquid media. R is the radius of the container and r represents the distance from the point where measurement was taken to the center of the container. Results suggest that as the distance to the base of the container increases, the velocity ratio in the Oz path tends to increase for both frequencies of the mechanical vibrator (15 Hz (\blacktriangle) and 35 Hz (\bullet)). However, the increase is more evident for the higher mechanical vibrator frequency of 35 Hz (\bullet). Moreover, for every considered distance from the vessel base, the particles direction in Oz path suffers an inversion when evaluated from the vessel wall to the sonotrode, as presented in Fig. 4. In fact, for both frequencies the velocity ratio is negative close to the acoustic radiator and positive near the container wall. Besides, as the distance to the base of the container increases the inversion direction point tends to move away from the acoustic radiator and is more evident for the height of $Z = 90$ mm, as represented in Fig. 4(c), which suggests that near the surface there is a large volume in which the velocity ratio is in negative direction (from the liquid to the surface). This is an important fact for the degassing process of liquid melt.

Regarding the Ox path the particles direction change with the frequency of the mechanical vibrator. Near the base of the

container and a frequency of 35 Hz (\circ) combined with $19,800 \pm 0.25$ Hz of ultrasound, the particles motion is always in the Ox positive direction (from the wall to the acoustic radiator), as we can see in Fig. 4(a). However, as the distance to the base of the container increases to $Z = 90$ mm, the particles motion tends to experiment an inversion. For 15 Hz (Δ) combined with $19,800 \pm 0.25$ Hz of ultrasound for every evaluated distance, the particles motion always present an inversion point as we can see from Fig. 4(a) to 4(c).

Through the results evaluated in Oz and Ox paths promoted by the combined effects (low and high vibration) in the medium, recorded by the high speed digital camera video and LDA equipment, the flow direction profile in the container can be suggested as presented in Fig. 5. Thus, the results obtained from this series of trials show that it is possible to have a soft agitation of the liquid through their own acoustic radiator, forcing the volume of liquid to pass in the zone of highest intensity of cavitation, i.e., close to the acoustic radiator which suggests that this technique can significantly increase the efficiency of ultrasonic degassing. Also, and in accordance with the results, the velocity of the flow is related with the free space/volume in the container (space/volume between the sonotrode and the container walls) and the length of sonotrode dipped in the fluid, which was the same for both stages of the present work and is according to similarity criteria presented in section 2.3.

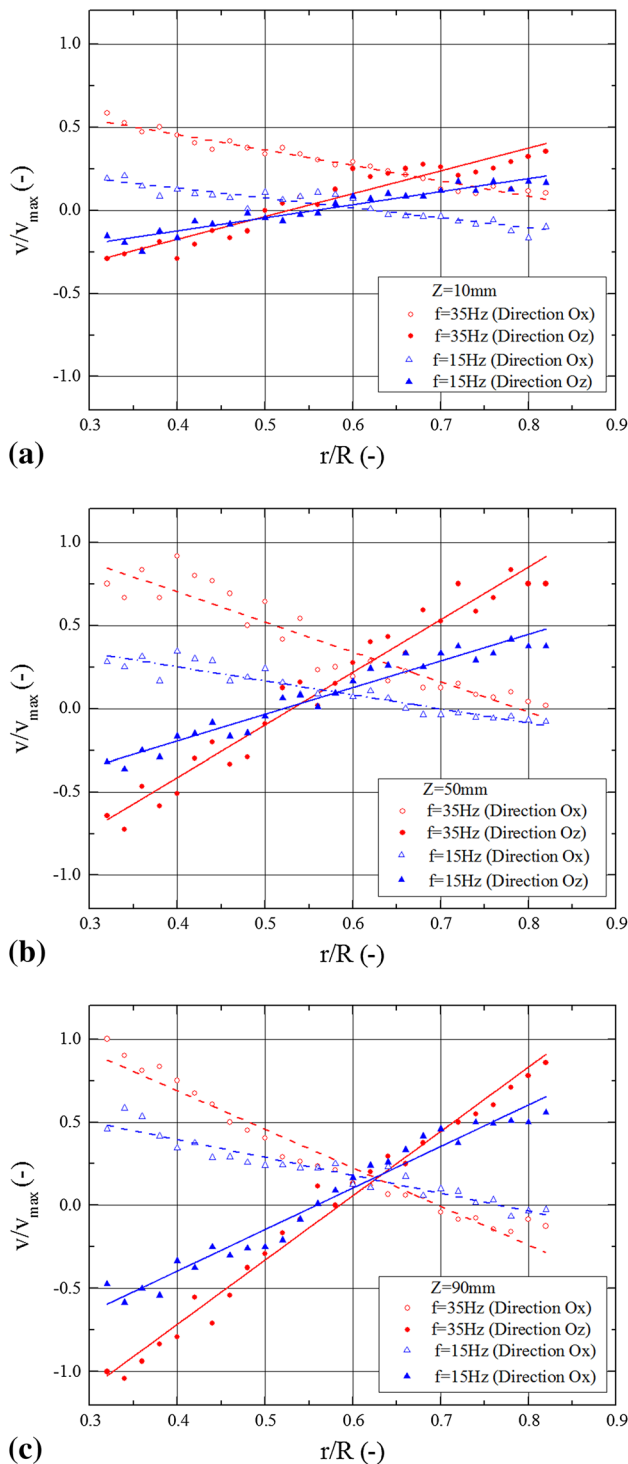


Fig. 4 Velocity ratio of the particles promoted by combination of effects at different points in the Ox and Oz directions: (a) $Z = 10$ mm; (b) $Z = 50$ mm; and (c) $Z = 90$ mm

3.2 Experiments in Liquid Aluminum

3.2.1 Effect of the New Degassing Approach on the H_2 Content. In an ideal melt, the viscosity and thermal conductivity are the main attenuation factors by losses of oscillation energy in the medium. However, in molten commercial aluminum alloy, the effect of impurities should also be

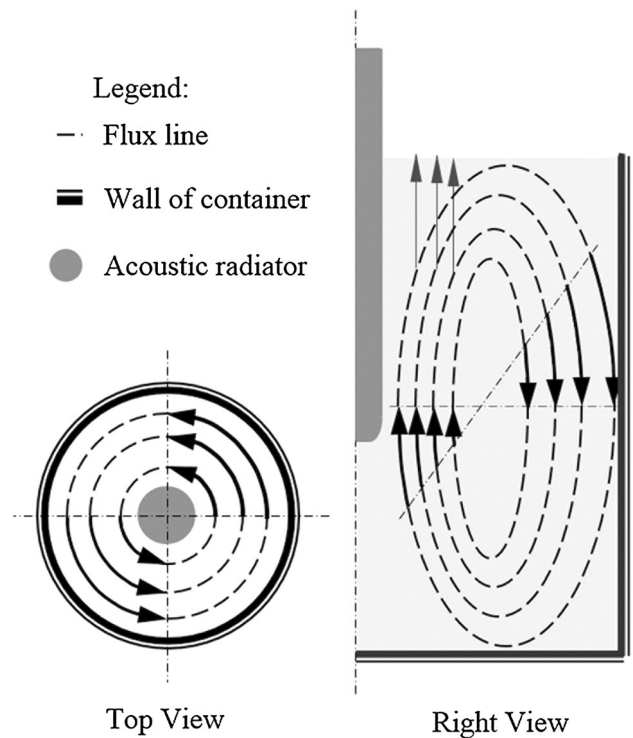


Fig. 5 Flow pattern induced by the MMM ultrasonic system

considered. In fact, the contact of the acoustic wave with impurities presents in liquid medium, typically oxides and non-metallic inclusions (Ref 10, 20), may result in a decrease of the acoustic intensity by the effect of ultrasound scattering, according to Eq 3. Furthermore, not all the cavitation bubbles reach the melt surface since part of them are transported by acoustic streaming to the bulk melt and often collapse, making the gases inside them to dissolve again in the molten alloy (Ref 21). This mechanism tends to slow down the process of ultrasonic degassing and to limit the maximum achieved value of alloy density.

Thus, according to the experimental results obtained in water, a similar motion profile may be imposed in the AlSi9Cu3(Fe) alloy melt by the combined effect of low and ultrasonic vibration, overcoming the limitations of the simple application of ultrasound, since a much greater volume of liquid metal is forced to pass near the acoustic radiator, where a well-developed cavitation regime occurs.

Figure 6 and 7 show the hydrogen content evolution for different processing times, at 660 and 700°C, respectively, with and without combination of effects and different degassing techniques. Regardless temperature, results show that this new degassing approach of molten aluminum, combining low frequency mechanical vibrator and US vibration, is clearly more efficient on the hydrogen removal rate than any other concurrent technique based in purging gas or just ultrasound (2). Moreover, the improvement in the degassing efficiency achieved by the combined effect when compared with the simple US degassing technique is more evident for temperatures below of 700°C (Fig. 6 and 7), which makes it possible to perform melt degassing at lower temperatures than usual. This is an extremely important issue for the casting practice since high degassing and/or pouring temperatures are directly related

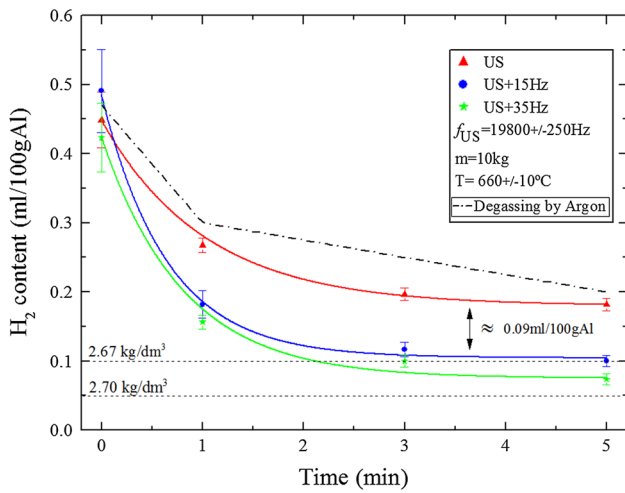


Fig. 6 Variation of hydrogen with degassing time at 660°C, for different degassing techniques

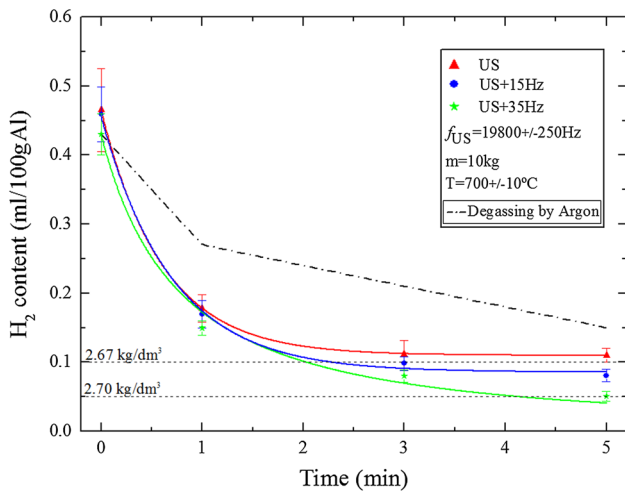


Fig. 7 Variation of hydrogen with degassing time at 700°C, for different degassing techniques

to high levels of hydrogen absorption, thus low degassing rates and final alloy density.

The theoretical density of this alloy is 2.74 kg/dm³, according to the supplier. For the combination of 19,800 ± 0.25 Hz with 35 Hz at 660°C (Fig. 6), the minimum amount of hydrogen in the medium after 5 min was 0.07 mL/100 g Al which corresponds to a density of 2.68 kg/dm³. On the other hand, for 700°C the minimum hydrogen content achieved was 0.04 mL/100 g Al which corresponds to a density higher than 2.7 kg/dm³ (Fig. 7). When compared with the single effect of ultrasound or argon technique, this new approach increased the degassing rate for both 15 and 35 Hz frequency of the mechanical vibrator. Besides, from Fig. 6 and 7, it is clear that although the curves present similar developments (exponential decay), the steady-state plateau that is reached is lower for the combined technique, which suggests that an effective stirring movement induced by this approach in the bulk liquid promoted its movement into the center of the crucible. For both degassing temperatures, both the simple US degassing technique and the combination of US and mechanical

vibration lead to a much higher degassing rate and much lower final hydrogen content in the melt.

The present results can be confirmed by the study conducted in water, in which the combined effect creates a liquid motion profile favorable to the passage of a large volume of metal in the area of greater acoustic activity (close to the US radiator), as well as by the sound pressure measurements presented in Fig. 8, obtained by an acoustic sensor developed in previous work (Ref 22).

A short sample of acoustic cavitation recording was saved for two different distances from the acoustic radiator, during the combined effect degassing process. This process was repeated ten times for each distance to reduce random errors. According to the results shown in Fig. 8, it is clear that the sub-harmonic (●) significantly decreases when the distance to the acoustic radiator increases. Besides the intensity of the FFT sub-harmonic (●) increase in areas close to the acoustic radiator, the intensity of the FFT ultra-harmonics (▲) seems to stabilize which is a consequence of a well-developed cavitation regime as suggested by (Ref 11, 23). According to Fig. 8 and the behavior of the sub-harmonic and ultra-harmonics, it is suggested that at distances from the acoustic radiator below 40 mm there is a well-developed cavitation regime, which starts to decrease for higher distances, although it is still clear, but with lower intensity, at 70 mm from the radiator. At 85 mm from the radiator, cavitation seems to be at its limit, or being even insipient, because the intensity of the sub-harmonic is quite low and the ultra-harmonics have already difficulty to stabilize on a clearly established value, thus acoustic streaming can perhaps be the most relevant acoustic phenomena in that region.

3.3 Effect of the New Degassing Approach in the Mechanical Properties

It is well known that mechanical properties of Al-Si alloys depend on several factors, with particular emphasis to microstructure morphology (Ref 24) and size and distribution of porosities (Ref 25-27). Porosity can be attributed to the inadequate feeding associated to volumetric shrinkage of liquid during solidification and/or to the decrease of hydrogen solubility in Al during cooling. Thus, reducing the content of hydrogen dissolved in the liquid metal (degassing operation) will have a significant impact in the alloys porosity, thus in their mechanical properties.

The results of mechanical characterization are presented in Fig. 9. It is clear that regardless the degassing technique, those alloys degassed at higher temperature (700°C) show higher tensile strength (UTS) and elongation to failure. This is mainly due to the most effective degassing operation and low porosity of the alloys degassed at higher temperature, as a consequence of the principle—the higher the melt temperature, the lower is the viscosity of the melt. In those alloys degassed by US or by the new technique, at lower temperatures, mainly below 700°C, the melt high viscosity hampers the pulsation of the cavitation bubbles, their coagulation and floating, as reported in previous research works (Ref 1, 2). Moreover, the diffusion coefficient of hydrogen in liquid metals decreases with decreasing temperature thus decreasing the diffusion rate of hydrogen from the solution to the bubbles. In those alloys degassed by argon purging only the last effect is present.

The ultrasonic degassing technique is more effective than gas purging for both melt temperatures, since it leads to higher

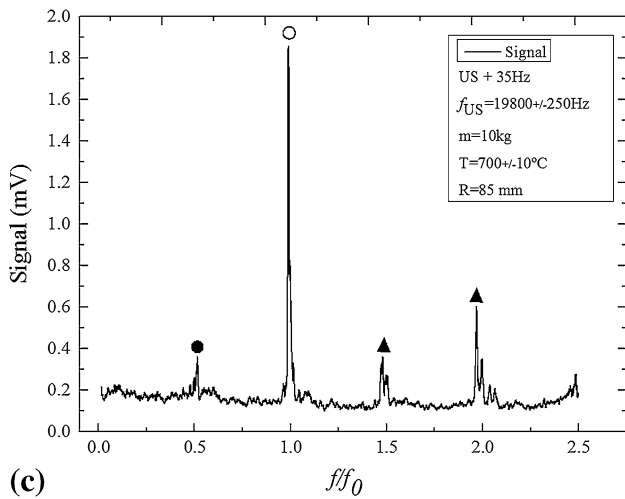
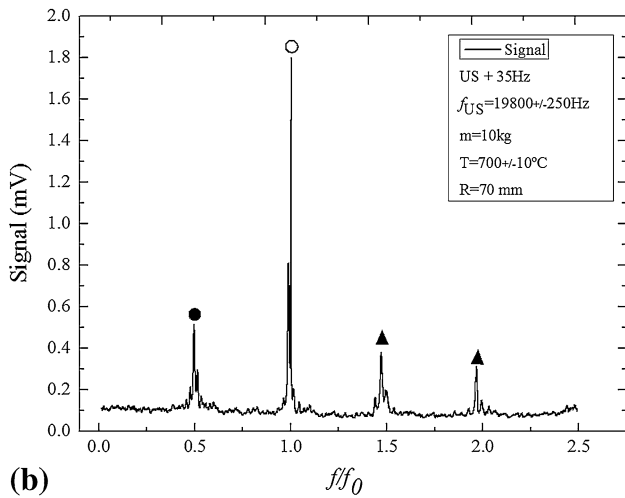
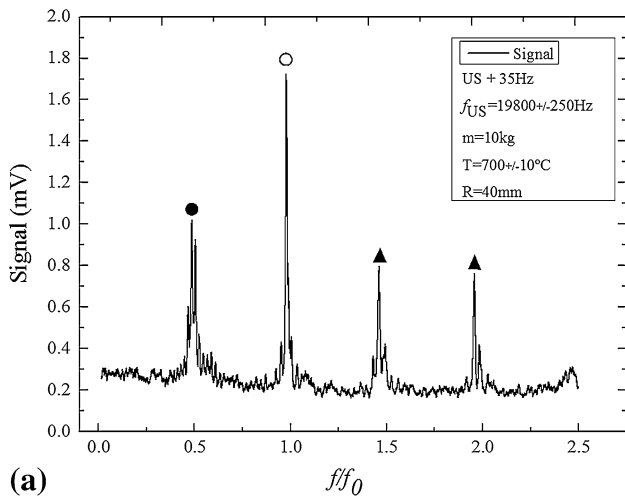


Fig. 8 FFT spectral levels of harmonics (○), sub (●), and ultraharmonics (▲) of acquired sound pressure waveform at different distances from the acoustic radiator, during the combined effect degassing process: (a) $R = 40\text{ mm}$ —distances from the acoustic radiator; (b) $R = 70\text{ mm}$ —distances from the acoustic radiator. (c) $R = 85\text{ mm}$ —distances from the acoustic radiator

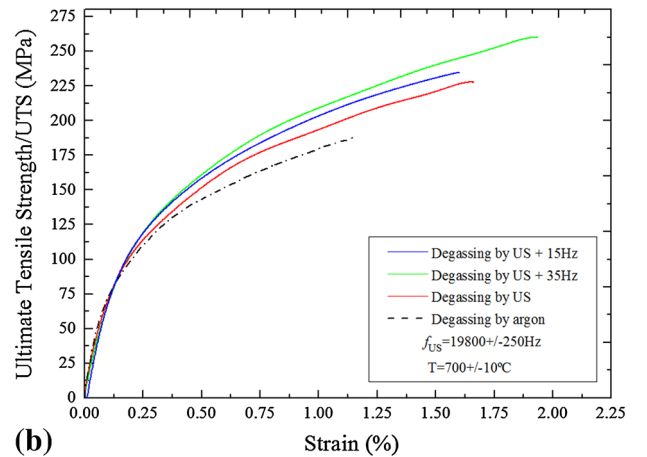
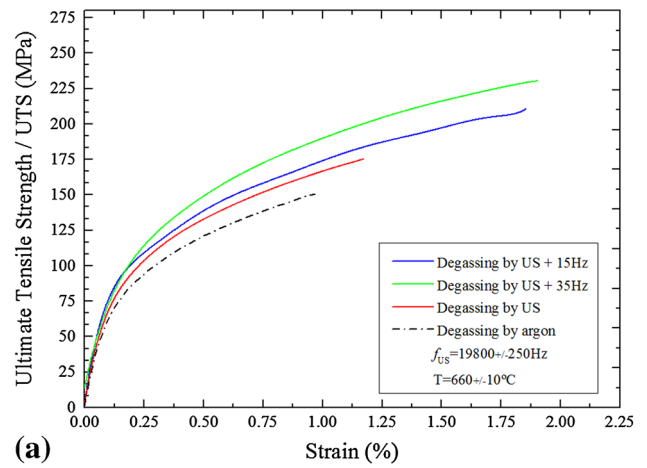


Fig. 9 Results of mechanical characterization of alloys degassed at (a) lower temperature (660° C) and (b) higher temperature (700° C)

mechanical properties (Fig. 9). In those samples degassed by gas purging, UTS and elongation to failure were 150 MPa and 1%, respectively, for 660° C melt temperature and 187 MPa and 1.13%, respectively, for 700° C melt temperature. These properties are significantly increased when degassing is performed by ultrasound—225 MPa and 1.61%, respectively, for 700° C melt temperature—and increase even more if ultrasonic degassing is combined with low frequency vibration of the molten alloy, using the new set-up. The highest values of UTS and elongation to failure were obtained for a combination of US degassing in the conditions presented in section 2.2 with 30 Hz mechanical vibration—262 MPa and 1.93%, respectively—for 700° C melt temperature.

According to these results, the new approach for aluminum degassing is a significant improvement over ultrasonic processing. UTS is 40 and 16.5% higher than in samples degassed by argon purging and by US, respectively, while elongation to failure is 71 and 20% higher, respectively.

In this experimental work, grain refinement and silicon modification has not been carried out, suggesting that the difference in mechanical properties between US degassed samples and those degassed using the new technique is mainly due to a difference in porosity. The best efficiency of the new

process can be attributed to the higher quantity of molten alloy that passes in the neighborhood of the acoustic radiator (the zone of higher acoustic activity) due to the melt stirring action promoted by the low mechanical vibrator, as described in section 3.1. Thus, as a result of melt stirring, cavitation bubbles developed in a higher volume of metal, improving degassing. Moreover, according to the findings in the experiments carried out in water, the molten alloy is forced to pass in the high acoustic activity repeatedly, meaning that the same liquid metal is submitted to high cavitation more than once, also improving the degassing efficiency.

4. Conclusions

The undertaken research proves to be an important contribution to understand how ultrasonic cavitation can be used to degas large volumes of aluminum melts. Thus, the following conclusions can be drawn:

1. When performing US degassing of liquid aluminum it is possible to induce melt stirring in the molten pool by coupling a mechanical vibrator to the sonotrode, using a suitable interface;
2. Melt stirring improves US degassing of aluminum alloys increasing the alloy density and the degassing rate;
3. The frequency of the mechanical vibrator is an important factor in the velocity and motion profile of the liquid media, and for the used set-up the best values were obtained for 35 Hz.
4. With the combined technique, it is possible to achieve alloy densities close to 2.7 kg/dm^3 after 5 min processing, while with simple US degassing only 2.66 kg/dm^3 has been achieved for the same processing conditions (700°C , 5 min).
5. The developed degassing technique increases the alloy tensile strength and strain when compared with traditional ultrasonic and argon purging techniques.

Acknowledgments

This research was supported by FEDER/COMPETE funds and by national funds through FCT - Portuguese Foundation for Science and Technology and was developed on the aim of the research Project PTDC/EME-TME/119658/2010 and the Post-Doctoral Grant SFRH/BPD/76680/2011. Acknowledgements also to the University of Minho, for the provision of research facilities.

References

1. H. Puga, J. Barbosa, E. Seabra, S. Ribeiro, and M. Prokic, The Influence of Processing Parameters on the Ultrasonic Degassing of Molten AlSi9Cu3 Aluminium Alloy, *Mater. Lett.*, 2009, **63**(9–10), p 806–808
2. H.B. Xu, X.G. Jian, T.T. Meek, and Q.Y. Han, Degassing of Molten Aluminum A356 Alloy Using Ultrasonic Vibration, *Mater. Lett.*, 2004, **58**(29), p 3669–3673

3. L. Moraru, Viscosity of a Eutectic Silumin Alloy in Ultrasonic Field and Estimation of Melting Temperature, *Indian J. Pure Appl. Phys.*, 2007, **45**(9), p 733–738
4. L. Moraru and M. Vlad, Nucleation of Crystals in Undercooled Molten Aluminium, *Revista de Chimie-Bucharest-Original Edition*, 2007, **58**(2), p 129–132
5. H. Puga, J. Barbosa, S. Costa, S. Ribeiro, A.M.P. Pinto, and M. Prokic, Influence of Indirect Ultrasonic Vibration on the Microstructure and Mechanical Behavior of Al–Si–Cu Alloy, *Mater. Sci. Eng. A*, 2013, **560**, p 589–595
6. L. Qingmei, Z. Yong, S. Yaoling, Q. Feipeng, and Z. Qijie, Influence of Ultrasonic Vibration on Mechanical Properties and Microstructure of 1Cr18Ni9Ti Stainless Steel, *Mater. Des.*, 2007, **28**(6), p 1949–1952
7. G. Timelli, P. Ferro, and F. Bonollo, Influence of Vibration During Solidification of Aluminium Metal Matrix Composites on Microstructure, *Metallurgia Italiana*, 2010, **102**(1), p 1–11
8. G.I. Eskin, Cavitation Mechanism of Ultrasonic Melt Degassing, *Ultrason. Sonochem.*, 1995, **2**(2), p 137–141
9. A.R.N. Meidani and A.M. Hasan, A Study of Hydrogen Bubble Growth During Ultrasonic Degassing of Al–Cu Alloy Melts, *J. Mater. Process. Technol.*, 2004, **147**(3), p 311–320
10. G.I. Eskin, *Ultrasonic Treatment of Light Alloy Melts*, Gordon and Breach Science, Amsterdam, 1998
11. O.V. Abramov, *High-Intensity Ultrasonics Theory and Industrial Applications*, Gordon and Breach Science, Amsterdam, 1998
12. G.I. Eskin, Principles of Ultrasonic Treatment: Application for Light Alloys Melts, *Adv. Perform. Mater.*, 1997, **4**(2), p 223–232
13. T.G. Leighton, Bubble Population Phenomena in Acoustic Cavitation, *Ultrason. Sonochem.*, 1995, **2**(2), p 123–136
14. J.W. Li, T. Momono, Y. Tayu, and Y. Fu, Application of Ultrasonic Treating to Degassing of Metal Ingots, *Mater. Lett.*, 2008, **62**(25), p 4152–4154
15. M. Prokic, Multifrequency Ultrasonic Structural Actuators, European Patent Application EP12387152001
16. H. Puga, J. Barbosa, D. Soares, F. Silva, and S. Ribeiro, Recycling of Aluminium Swarf by Direct Incorporation in Aluminium Melts, *J. Mater. Process. Technol.*, 2009, **209**(11), p 5195–5203
17. D.V. Neff, *Nonferrous Molten Metal Processes*, ASM Metals Handbook, Metal Parks, 1989
18. M. Saternus and J. Botor, Refining Process of Aluminium Conducted in Continuous Reactor—Physical Model, *Arch. Metall. Mater.*, 2010, **55**(2), p 463–475
19. M. Saternus, Influence of Impeller Shape on the Gas Bubbles Dispersion in Aluminium Refining Process, *J. Archiv. Mater. Manuf. Eng.*, 2012, **55**(2), p 285–290
20. D. Dispinar, S. Akhtar, A. Nordmark, M. Di Sabatino, and L. Amberg, Degassing, Hydrogen and Porosity Phenomena in A356, *Mater. Sci. Eng. A*, 2010, **527**(16–17), p 3719–3725
21. H.B. Xu, Q.Y. Han, and T.T. Meek, Effects of Ultrasonic Vibration on Degassing of Aluminum Alloys, *Mater. Sci. Eng. A*, 2008, **473**(1–2), p 96–104
22. H. Puga, J. Barbosa, J. Gabriel, E. Seabra, S. Ribeiro, and M. Prokic, Evaluation of Ultrasonic Aluminium Degassing by Piezoelectric Sensor, *J. Mater. Process. Technol.*, 2011, **211**(6), p 1026–1033
23. K. Brabec and V. Mornstein, Detection of Ultrasonic Cavitation Based on Low-Frequency Analysis of Acoustic Signal, *Cent. Eur. J. Biol.*, 2007, **2**(2), p 213–221
24. M. Panuskova, E. Tillova, and M. Chalupova, Relation Between Mechanical Properties and Microstructure of Cast Aluminum Alloy AlSi9Cu3, *Strength Mater.*, 2008, **40**(1), p 98–101
25. Y.M. Li and R.D. Li, Effect of the Casting Process Variables on Microporosity and Mechanical Properties in an Investment Cast Aluminium Alloy, *Sci. Technol. Adv. Mater.*, 2001, **2**(1), p 277–280
26. A.M. Samuel and F.H. Samuel, Effect of Melt Treatment, Solidification Conditions and Porosity Level on the Tensile Properties of 319.2 Endchill Aluminum Castings, *J. Mater. Sci.*, 1995, **30**(19), p 4823–4833
27. M.K. Surappa, E. Blank, and J.C. Jaquet, Effect of Macro-Porosity on the Strength and Ductility of Cast Al-7Si-0.3Mg, *Scripta Metall.*, 1986, **20**(9), p 1281–1286